

Via Coupling within Power-Return Plane Structures Considering the Radiation Loss

Richard L. Chen, Ji Chen, Todd H. Hubing*, and Weimin Shi**

Department of Electrical and Computer Engineering
University of Houston, Houston, TX 77204

*Department of Electrical and Computer Engineering
University of Missouri-Rolla, Rolla, MO 65409

**Desktop Platform Group
Intel Corporation, Hillsboro, OR 97124

Abstract: An accurate analytical model to predict via coupling within rectangular power-return plane structures is developed. Loss mechanisms, including radiation loss, dielectric loss, and conductor loss, are considered in this model. The radiation loss is incorporated into a complex propagating wavenumber as an artificial loss mechanism. The quality factors associated with three loss mechanisms are calculated and compared. The effects of radiation loss on input impedances and reflection coefficients are investigated for both high-dielectric-loss and low-dielectric-loss PCBs. Measurements are performed to validate the effectiveness this model.

I. INTRODUCTION

Power and ground-plane noise, also known as simultaneous switching noise (SSN), inductive noise or Delta-I noise, can appear in printed circuit board (PCB) and multichip module (MCM) designs when a high-speed time varying or a transient current flows through a via [1]-[5]. Due to the via discontinuity, part of the power is transmitted into the substrate and coupled to other devices on the PCB. The signal coupled to other devices may cause signal integrity and electromagnetic compatibility (EMC) issues [1]-[5]. As the clock frequency increases and the rise time decreases, the likelihood of significant mutual coupling occurring between a via and its neighboring devices increases. The signal can also radiate into its environment and cause electromagnetic interference (EMI) problems [6]. Therefore, to ensure successful designs of high-speed electronic products, it is important to develop modeling techniques that can accurately estimate the mutual coupling between a via and its surrounding devices and predict the PCB radiation due to via discontinuities.

Power-return plane modeling has been carried out by using analytical methods [1]-[3] and full-wave techniques [4][5][7]. The analytical methods use either the radial waveguide model or the cavity model to extract the structure's input impedance or mutual impedance. The computational cost of analytical approaches is typically much less than that of the full-wave techniques and the underlying physical mechanism is also clearer. Therefore, an analytical approach is preferred

whenever it is possible. However, to our knowledge, existing analytical approaches ignore radiation loss in the input impedance or mutual impedance estimation. This approximation may lead to significant errors in the input impedance estimation for some PCB structures. In [6], the radiated field of a rectangular power-return plane structure was investigated as an electromagnetic interference problem, a strong radiation effect is observed at resonant frequencies. However, the effect of the radiation on the via input impedance or the mutual impedance were not studied. In [8], radiation effects on the input impedance were investigated for a circular PCB structure. In the model, the radiation loss is considered by introducing a non-zero surface admittance around the cavity and is calculated using the spectral domain immittance (SDI) approach [9]. The results showed that the radiation loss cannot be neglected at the resonant frequencies, particularly for thick substrate PCBs. Unfortunately, this approach is not directly applicable to the via discontinuity analysis for general power-return plane structures since the constant edge impedance assumption is not valid for practical rectangular structures.

The purpose of this paper is to introduce a more general approach to include the radiation loss in analyzing practical rectangular power-return plane structures. Rather than calculating the location- and mode-dependent edge impedance on the periphery of the power-return plane [10], the effect of the radiation loss is accounted for by assuming an equivalent loss in the complex propagating wavenumber. The radiation loss is calculated by integrating the radiation fields of equivalent magnetic currents on the edges of the PCBs. As discussed in [3], in high-loss power-return plane structures, where the board resonance is significantly damped, the input impedance is an upper bound on the transfer impedance between any two points on the board. Hence, in this paper, only the input impedance is studied as the worst case scenario.

The remainder of the paper is organized as following. Section II describes the development of the input impedance model that includes dielectric loss, conductive loss, and radiation loss. The procedure for calculating the radiation loss quality factor is described in Section III. In Section IV, the

approach is applied to analyze the input impedance/reflection coefficients of two typical power-return plane structures and results are compared with experimental data. Conclusions are given in Section V.

II. INPUT IMPEDANCE MODEL

A typical rectangular power-return plane structure is shown in Fig. 1. It consists of two metal plates with length, l , and width, w , and a dielectric slab (with a thickness of h) sandwiched between the two metal plates. The metal plates have a conductivity of σ and the substrate has a relative dielectric constant of ϵ_r and a loss tangent of $\tan\delta$. A via with a radius of r_0 is located at (x_0, y_0) and a current source I is impressed into the via.

The power-return plane can be approximated by a cavity model where the top and bottom walls are perfect electric conductor (PEC) walls and the four side walls are perfect magnetic conductor (PMC) walls [11]. Since the substrate is electrically thin, only the transverse magnetic (TM) modes need to be considered [11]. To account for the fringing effects, an effective length, $l_e = l + h/2$ and an effective width, $w_e = w + h/2$, are used. More accurate empirical models for the effective length/width are available in [12][13], but they are derived for the dominant mode and assumed to work for other modes. Therefore, the simplified effective length-width model is used in this study.

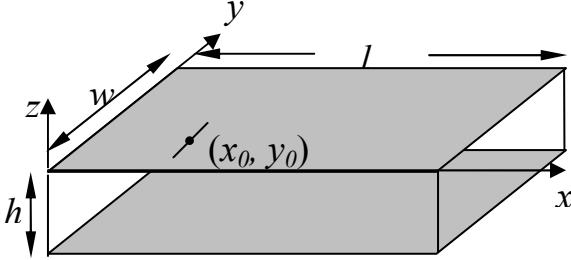


Figure 1. A rectangular power-return plane structure.

The electric field in the rectangular cavity can be written as [11]

$$E_z(x, y) = \sum_{m=0}^{\infty} \sum_{n=0}^{\infty} A_{mn} \psi_{mn}(x, y), \quad (1)$$

where

$$\psi_{mn}(x, y) = \cos\left(\frac{m\pi x}{l_e}\right) \cos\left(\frac{n\pi y}{w_e}\right) \quad (2)$$

represents a cavity mode (TM_{mn}) supported by the structure. The corresponding excitation coefficient is determined by the inner product of the mode and the source, shown as

$$A_{mn}(x, y) = \frac{j\omega\mu \langle J_z, \psi_{mn} \rangle}{\langle \psi_{mn}, \psi_{mn} \rangle} \frac{1}{k_{1e}^2 - k_{mn}^2}, \quad (3)$$

where J_z is the driving current density, $k_{mn} = \sqrt{\left(\frac{m\pi}{l_e}\right)^2 + \left(\frac{n\pi}{w_e}\right)^2}$, and k_{1e} is the effective wave number given by [14]

$$k_{1e} = k_1 \sqrt{1 - jL_s}. \quad (4)$$

In (4), $k_1 = \omega\sqrt{\mu\epsilon_r\epsilon_0}$ and L_s is the total loss due to three loss mechanisms, including the conductor loss, the dielectric loss and the radiation loss. It is given by [14]

$$L_s = \frac{1}{Q} = \frac{1}{Q_c} + \frac{1}{Q_d} + \frac{1}{Q_r}, \quad (5)$$

where Q stands for the total quality factor, and Q_c , Q_d , and Q_r represent the quality factors of the conductor loss, the dielectric loss, and the radiation loss. The conductor and dielectric loss quality factors can be written as

$$Q_d = \frac{1}{\tan\delta} \quad (6)$$

and

$$Q_c = \frac{h}{\delta_s}, \quad (7)$$

where δ_s is the skin depth, given as

$$\delta_s = \sqrt{\frac{2}{\omega\mu\sigma}}. \quad (8)$$

Assuming the total loss, $L_s \ll 1$, which is true for most of the substrate due to the narrow-band nature of power-return plane structures, applying the binomial expansion yields:

$$k_{1e} = k \left(1 - j \frac{\tan\delta + \frac{\delta_s}{h}}{2} - j \frac{1}{2Q_r} \right). \quad (9)$$

As shown in the above equation, the three loss mechanisms are represented by the imaginary parts in the complex wavenumber. Neglecting the radiation loss ($Q_r = \infty$) yields the complex wavenumber given in [1][16], which is valid when the dielectric loss or the conductor loss is dominant. However, when the substrate is thick or low loss, the assumption is no longer valid and the radiation loss has to be taken into consideration.

The impressed current on the via can be equivalently represented by a strip of current with a width of w_s , where $w_s = e^{2/3} r_0$ [15]. Hence, the driving current density can be obtained by

$$J_z = \frac{I}{w_s} \quad (10)$$

Substituting (9) and (10) into (3) and then substituting (3) into (1), one can obtain the input impedance as

$$Z_{in} = -\frac{E_z h}{I} = -\frac{j\omega\mu h}{I^2} \sum_{m=0}^{\infty} \sum_{n=0}^{\infty} \frac{\langle J_z, \psi_{mn} \rangle^2}{\langle \psi_{mn}, \psi_{mn} \rangle} \frac{1}{k_{1e}^2 - k_{mn}^2}, \quad (11)$$

where

$$\langle J_z, \psi_{mn} \rangle = I \text{sinc} \left(\frac{n\pi w_s}{2w_e} \right) \cos \left(\frac{m\pi x_0}{l_e} \right) \cos \left(\frac{n\pi y_0}{w_e} \right) \quad (12)$$

and

$$\langle \psi_{mn}, \psi_{mn} \rangle = \frac{w_e l_e}{4} (1 + \delta_{m0})(1 + \delta_{n0}). \quad (13)$$

In (13), δ_{n0} is defined as $\delta_{n0} = \begin{cases} 1 & \text{for } n = 0 \\ 0 & \text{for } n \neq 0 \end{cases}$. From (6) and (7), the dielectric loss and conductor loss can be obtained directly. However, the radiation loss, Q_r , still needs to be evaluated. In the next section, the steps to calculate the radiation quality factor, Q_r , are described.

III. EVALUATION OF QUALITY FACTOR FOR RADIATION LOSS

The radiation loss Q_r in (9) can be determined by using

$$Q_r = \omega \left(\frac{U_s}{P_r} \right) \quad [17], \text{ where } U_s \text{ is the electromagnetic energy}$$

stored inside the cavity and P_r is the power radiated from the cavity. The radiation loss quality factor only needs to be evaluated at the power-return plane's resonant frequencies since the electric field in low loss cavities is much stronger at these frequencies than that at the off-resonance frequencies, as indicated in (3). At the resonant frequency f_{mn} , the total electric field can be approximated by the resonant mode TM_{mn} as [6]

$$E_z(x, y) \approx A_{mn} \cos \left(\frac{m\pi x}{l_e} \right) \cos \left(\frac{n\pi y}{w_e} \right). \quad (14)$$

With this electric field distribution, the stored energy is obtained by

$$\begin{aligned} U_s &= 2U_E \\ &= 2 \iiint_V \frac{1}{4} \epsilon_0 \epsilon_r |E_z|^2 dV \\ &= \frac{1}{8} \epsilon_0 \epsilon_r h |A_{mn}|^2 (1 + \delta_{m0})(1 + \delta_{n0}), \end{aligned} \quad (15)$$

and the radiated power can be obtained by

$$P_{sp} = \int_0^{2\pi} \int_0^\pi S_r(r, \theta, \varphi) r^2 \sin \theta d\theta d\varphi, \quad (16)$$

where $S_r(r, \theta, \varphi) = \frac{1}{2\eta_0} \left[|E_\theta|^2 + |E_\varphi|^2 \right]$ is the magnitude of

Poynting vector. The value of $S_r(r, \theta, \varphi)$ can be determined by integrating the equivalent magnetic currents ($\vec{M}_s = -\hat{n} \times \vec{E}$) on the edges of the cavity as described in the Appendix A [6]. Once the U_s and P_r are obtained, the effect of radiation loss on the input impedance can be evaluated.

IV. NUMERICAL AND EXPERIMENTAL RESULTS

In this section, the developed modeling technique is applied to two typical power-return plane structures. The section starts

with an investigation and comparison of the three types of quality factors. Then the input impedance/reflection coefficient is calculated and also validated by experimental results.

A. Quality factors

To investigate the importance of radiation effects on input impedance, the quality factor, Q_r , needs to be compared with the other two quality factors, Q_c and Q_d . The first example considered here is a FR4 test board with a dimension of $16 \times 10 \times 0.127 \text{ cm}^3$. The substrate has a relative dielectric constant of 3.84 and a loss tangent of 0.019. The board is fed by a SMA connector (with an inner radius of $6.25 \times 10^{-2} \text{ cm}$) at the location $x_0 = 4.0 \text{ cm}$ and $y_0 = 5.0 \text{ cm}$. The conductivity of copper used for the calculations was $5.813 \times 10^7 \text{ S/m}$. The quality factors for all three loss mechanisms are shown in Figure 2. For this board, the dominant loss is the dielectric loss ($Q_d = 52.6$), which is assumed to be a constant over the entire frequency range. The quality factor associated with the conductor loss increases proportional to the square root of frequency, and is in the range of hundreds. The quality factor associated with the radiation loss varies from hundreds to thousands depending on the resonant cavity modes. In general, it is observed that radiation losses associated with modes with $m \neq 0$ and $n \neq 0$ (such as TM_{11} , TM_{21} and TM_{12} modes) are much smaller than that of other modes (such as TM_{01} , TM_{20} , TM_{30} and TM_{02} modes) with the exception of TM_{10} mode. For TM_{02} mode, the radiation loss quality factor goes as low as 171.2. For this mode, the radiation loss must be considered in the modeling.

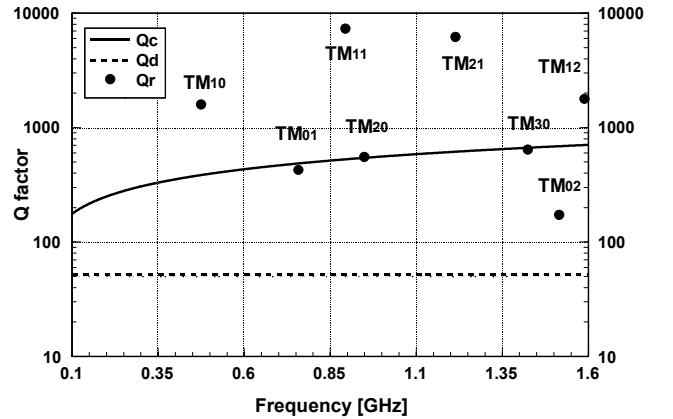


Figure 2. Calculated quality factors for a $16 \times 10 \times 0.127 \text{ cm}^3$ power-ground plane structure filled with FR4.

The three loss mechanisms are then investigated as a function of substrate thickness. Figure 3 shows the quality factors of TM_{20} and TM_{02} modes versus substrate thickness at the resonant frequencies. Again, the dielectric loss is independent of substrate thickness and modes. The conductor quality factor increases when the substrate becomes thicker for both TM_{20} and TM_{02} modes as expressed in (7). As the substrate thickness increases, the magnitude of the equivalent

edge magnetic current increases and hence more power is radiated into the free space. As a result, the radiation quality factor decreases correspondingly. Depending on the operating frequency, the operating mode and the substrate thickness, the radiation loss could be very important to power-return plane structures.

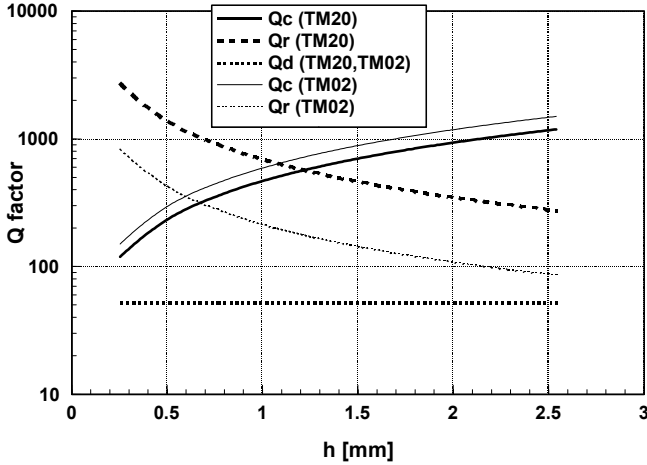


Figure 3. Quality factors versus substrate thickness for a $16\text{ cm} \times 10\text{ cm}$ power-ground plane structure filled with FR4 at the TM_{20} mode and TM_{02} resonances.

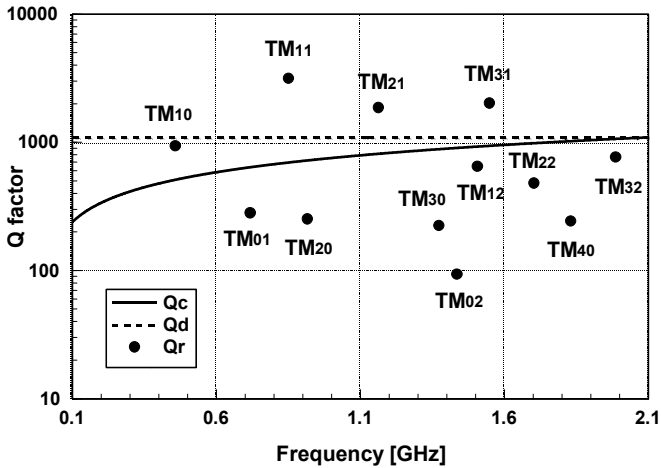


Figure 4. Quality factors for a $22 \times 14 \times 0.15748\text{ cm}^3$ power-ground plane structure filled with Rogers RT/duroid 5880.

The second example considered here is a low-dielectric-loss high frequency material, RogersTM RT/duroid 5880. The board size is $22\text{ cm} \times 14\text{ cm}$. The substrate is 0.15748 cm (62 mil) thick with a dielectric constant of 2.2 and a loss tangent of 0.0009. Figure 4 shows a plot of the three quality factors as a function of frequency. In this case, the dielectric loss is very low, and hence the radiation loss and conductor loss become dominant factors. In addition, due to the thick substrate, the radiation loss can be much larger than the conductor loss at several resonant frequencies. For example, at the TM_{02}

resonance, the radiation quality factor is less than 100, which is far more important than both conductor loss and dielectric loss. Therefore, radiation loss must be considered for input impedance calculation. It is also observed that the radiation loss of modes with $m \neq 0$ and $n \neq 0$ is much less than that of other modes with either $m = 0$ or $n \neq 0$, except for TM_{10} mode.

Based on the above discussion, one can conclude that the radiation loss is closely related to the substrate thickness and cavity modes. They can become dominant for low dielectric loss substrates.

B. Input impedance

Once the quality factors are obtained, the effective wavenumber can be calculated from (4) and (5). Substituting the effective wavenumber into (11) yields the input impedance of a rectangular power-return structure. The input impedance of the FR4 board, which was described earlier, is studied first. The magnitude of input impedance is shown in Figure 5. Only four modes are excited within the simulated frequency range due to the excitation position. Since the dominant dielectric loss is very strong, the radiation loss can be neglected for most of the modes, except for TM_{02} mode. For TM_{02} mode, neglecting the radiation loss can cause about 20% error in the input impedance estimation. This can be explained by comparing the quality factors of both dielectric loss and radiation loss for the TM_{02} in Fig. 2. As shown in Fig. 2, the radiation loss quality factor is only about three times that of the dielectric loss quality factor. Therefore, it contributes significantly to the input impedance estimation.

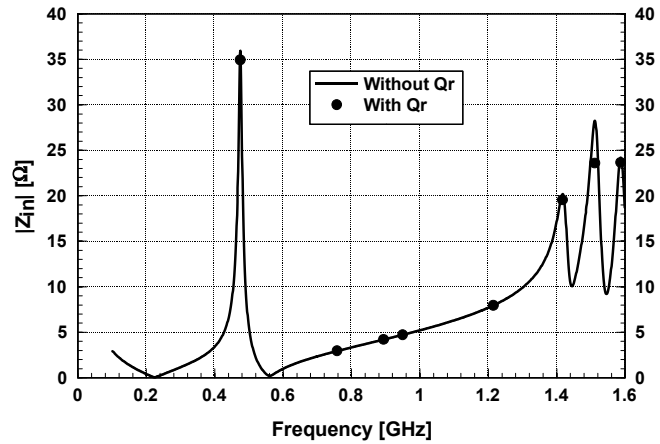


Figure 5. Input impedance of a $16 \times 10 \times 0.127\text{ cm}^3$ power-ground plane structure filled with FR4.

Next the RT/duroid board, which has a low dielectric loss is investigated. The via is located at $x_0 = 5.5\text{ cm}$ and $y_0 = 3.5\text{ cm}$. The reflection coefficient of the RT/duroid board is studied numerically and experimentally. The magnitude of reflection coefficient is shown in Figure 6. At this via

position, only seven modes are excited in a frequency range from 100 MHz to 2.1 GHz. As shown in the figure, without considering the radiation loss, the reflection coefficients are overestimated. This error could be significant depending on the operating modes, such as the 2nd mode shown in the figure. When the radiation loss is considered at resonance frequencies, a better agreement can be observed. Especially the first two modes, they match the measured data closely.

The figure also shows that the predicted resonance frequencies are lower than the measured resonance frequencies, especially at the high frequency end. It is due to the approximation of fringing field compensation. The fringing field consideration also affects the estimation of reflection coefficients at the resonant frequencies. In addition, the particular test board was cut manually, which may have an error on the order of the substrate thickness in both board width and length. Currently, we are developing mode-dependent model to approximate the fringing effect and investigating the application of impedance boundary condition to improve the accuracy of input impedance estimation at high frequencies.

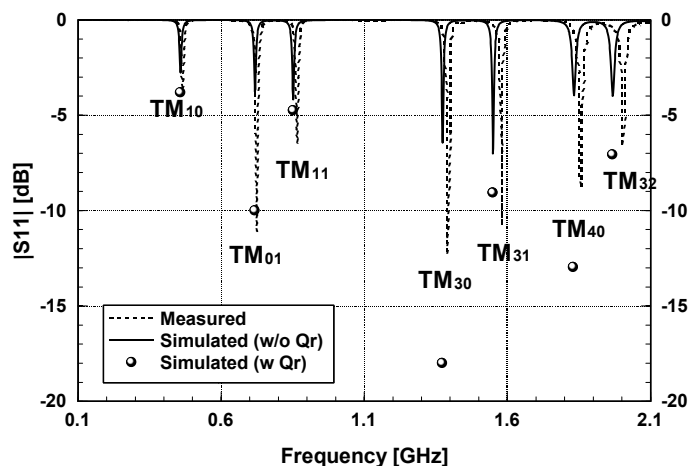


Figure 6. Reflection coefficients for a $22 \times 14 \times 0.15748 \text{ cm}^3$ power-ground plane structure filled with RogersTM RT/duroid 5880.

V. CONCLUSIONS

The radiation effect on via coupling in a rectangular power-return plane was studied. The radiation loss quality factor was investigated and compared to the dielectric loss and conductor loss quality factors. Numerical and experimental investigations were performed to demonstrate the radiation effects on via-to-substrate coupling for both high-dielectric-loss and low-dielectric-loss substrates. It was observed that without considering the radiation loss, the cavity model input impedance calculation can exhibit significant errors, especially for low-dielectric-loss PCBs. For thicker substrates, the radiation loss may become comparable to the dielectric loss, and hence radiation effects must be considered in order

to accurately predict the coupled noise. Results also show that the modes with $m \neq 0$ and $n \neq 0$ generally exhibited lower radiation loss than that of the modes with either $m = 0$ or $n = 0$. This suggests that via positions could be chosen to avoid exciting strong radiation modes in order to circumvent EMI problems.

REFERECES:

- [1] G. T. Lei, R. W. Techtent, and B. K. Gilbert, "High-frequency characterization of power/ground-plane structures," *IEEE Trans. Microwave Theory and Techniques*, vol. 47, pp. 562-569, May 1999.
- [2] J. C. Parker Jr., "Via coupling within parallel rectangular planes," *IEEE Trans. Electromagnetic Compatibility*, vol. 39, pp. 17-23, Feb. 1997.
- [3] M. Xu, T. H. Hubing, "The development of a closed-form expression for the input impedance of power-return plane structures," *IEEE Trans. Electromagnetic Compatibility*, vol. 45, pp. 478-485, Aug. 2003.
- [4] J. G. Yook, V. Chandramouli, L. P. B. Katehi, K. A. Sakallah, T. R., Arabi, and T. A. Schreyer, "Computation of switching noise in printed circuit boards," *IEEE Trans. Comp. Packag., Manufact. Technol.*, vol. 20, pp. 64-75, March 1997.
- [5] H. Liaw and H. Merkelo, "Simulation and modeling of mode conversion at vias in multilayer interconnects," in *Proc. IEEE 45th Elect. Comp. Technol. Conf.*, 1995, pp. 361-367.
- [6] M. Leone, "The radiation of a rectangular power-bus structure at multiple cavity-mode resonances," *IEEE Trans. Electromagnetic Compatibility*, vol. 45, pp.486-492, Aug. 2003.
- [7] W. Shi and J. Fang, "New efficient method of modeling electronics packages with layered power/ground planes," *IEEE Trans. Advanced Packaging*, vol. 25, pp. 417-423, Aug. 2002.
- [8] R. L. Chen and J. Chen, "Radiation effects on via coupling in power-return plane structures," *Microwave and Optical Technology Letters*, vol. 41, pp. 117-119, April 20, 2004.
- [9] T. Itoh, "Spectral domain immittance approach for dispersion characteristics of generalized printed transmission lines," *IEEE Trans. Microwave Theory and Techniques*, vol. 28, pp. 410-413, July 1980.
- [10] E. F. Kuester, R. T. Hohnk and D. C. Chang, "The thin-substrate approximation for reflection from the end of a slab-loaded parallel-plate waveguide with application to microstrip patch antennas," *IEEE Trans. Antennas and Propagation*, vol. 30, pp. 910-917, September 1982.
- [11] Y. T. Lo, D. Solomon, and W. F. Richards, "Theory and experiment on microstrip antennas," *IEEE Trans. Antennas and Propagation*, vol. 27, pp. 137-145, March 1979.
- [12] E. O. Hammerstad, "Equations for microstrip circuit design," *Proc. 5th European Microwave Conference*, 1975, pp.268-272.
- [13] M. Kara, "Formulas for the computation of the physical properties of rectangular microstrip antenna elements with various substrate thickness," *Microwave and Optical Technology Letters*, vol. 12, pp. 234-239, 1996.
- [14] D. R. Jackson, "Analysis techniques for microstrip antennas," Part II of short course on the analysis and design of microstrip antennas and arrays, *IEEE Antennas and Propagation Society International Symposium*, Chicago IL, July 1992
- [15] D. M. Pozar, "Improved computational efficiency for the moment method solution for printed dipoles and patches," *Electromagnetics*, vol. 13, pp. 299-309, 1983.
- [16] T. Okoshi, *Planar Circuits for Microwaves and Lightwaves*. New York: Springer-Verlag, 1985.
- [17] J. R. James, P. S. Hall and C. Wood, *Microstrip Antennas: Theory and Design*. Peter Peregrinus, Stevenage, U.K., 1981.

APPENDIX A EVALUATION OF RADIATED POWER FROM POWER-RETURN PLANES.

For completeness, the equations for the radiation power calculation are listed. They are developed in [6].

The far field from the power-return plane radiation can be described by

$$\vec{E} = A_{mn} h \frac{e^{-jk_0 r}}{4\pi r} (\vec{P}_L G_L S_L - \vec{P}_W G_W S_W), \quad (\text{A1})$$

where

$$\vec{P}_L = \sin \varphi \hat{\phi} + \cos \theta \cos \varphi \hat{\phi}, \quad (\text{A2})$$

$$\vec{P}_W = -\cos \varphi \hat{\phi} + \cos \theta \sin \varphi \hat{\phi}, \quad (\text{A3})$$

$$S_L = \frac{jk_0 k_\xi}{\left(\frac{m\pi}{l_e}\right)^2 - k_\xi^2} G_W, \quad (\text{A4})$$

$$S_W = \frac{jk_0 k_\eta}{\left(\frac{n\pi}{w_e}\right)^2 - k_\eta^2} G_L, \quad (\text{A5})$$

$$G_L = 1 - (-1)^n e^{jk_\eta w_e}, \quad (\text{A6})$$

$$G_W = 1 - (-1)^m e^{jk_\xi l_e}, \quad (\text{A7})$$

and

$$\begin{Bmatrix} k_\xi \\ k_\eta \end{Bmatrix} = k_0 \sin \theta \begin{Bmatrix} \cos \varphi \\ \sin \varphi \end{Bmatrix}. \quad (\text{A8})$$